

Experimental and numerical investigation of 2D sloshing with slamming

A. Colagrossi* C. Lugni* M. Greco* O. M. Faltinsen**
a.colagrossi@insean.it c.lugni@insean.it m.greco@insean.it oddfal@marin.ntnu.no

* INSEAN, Italian Ship Model Basin, Roma – Italy.

** Centre for Ships and Ocean Structures, NTNU, Trondheim – Norway.

Partially filled tanks can experience sloshing in several practical circumstances. This is a resonance phenomenon where the free-surface can highly deform. The liquid will move back and forth rising along the side walls, possibly impacting against the roof. Impact on a side tank wall may also occur, *e. g.* in shallow water conditions. Resulting slamming loads are of main concern. A synergic experimental–numerical investigation of the sloshing flows is currently performed. Here the main focus is on the occurrence of slamming events and on the prediction of the related loads. Numerically, our approach is based on the SPH method, introduced by Monaghan and coauthors (see Monaghan (1994)) and further developed by Colagrossi and Landrini (2003). Both single– and two–phase flow (gas and liquid) SPH models have been developed. This method is able to follow the whole flow evolution in the tank and handle the many relevant and complicated phenomena generally involved. Among those we can list: water run–up and run–down along the side walls, roof impacts, free-surface overturning and breaking onto the underlying water, air cushioning. Often these features characterize the flow for intermediate and shallow water depths which can establish in real tanks and are of interest in the present research activity. Experimentally a two-step investigation has started. We decided to reduce as much as possible the geometric complexities for a better understanding of the flow features. Therefore we consider the flow in a rigid square tank, as sketched in

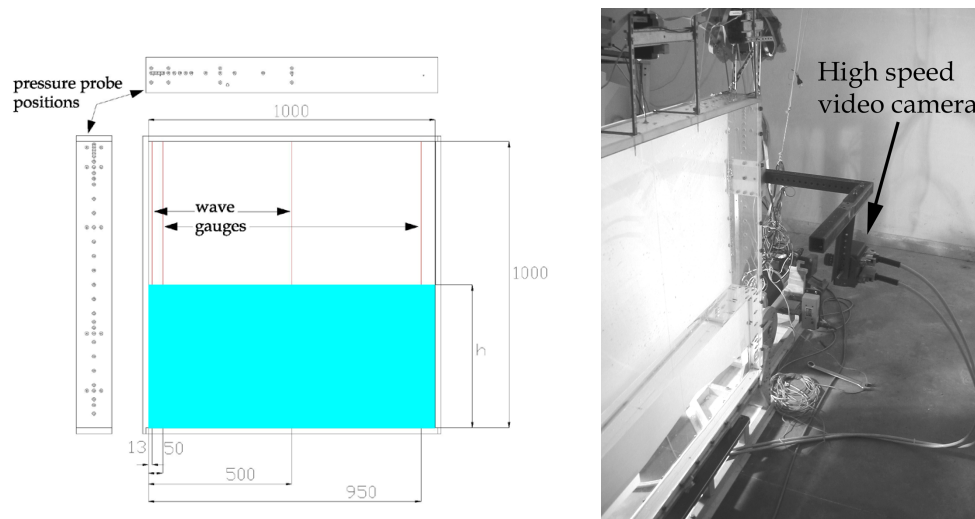


Figure 1: Left: sketch of the experimental set up. Wave gauge positions and possible pressure sensor locations are indicated. Dimensions are in millimeters. Right: partial side view of the experimental set-up. The high speed video camera is shown.

the left plot of figure 1. The tank is $L = H = 1$ m long and $b = 0.1$ m wide and is filled with water up to a height h . Due to the geometry, the flow inside the tank is two-dimensional in the main tank plane, unless flow instabilities are excited. A pure-sway is assumed as forced motion with sinusoidal law, $A \sin(2\pi t/T)$. Here A and T are the excitation amplitude and period, respectively. The tank was equipped with four wave gauges placed along its length to measure the water height evolution during sloshing phenomena. Twelve pressure sensors were located along the vertical side walls and the tank roof to predict the slamming loads acting on the structure. The experimental apparatus has been designed to vary the probe positions from run to run. In this way it is possible to reconstruct the pressure distribution induced on the walls by their interaction with the water flow. During the tests flow visualizations were performed through low and high speed digital video cameras with sampling frequency 23 Hz and 4000 Hz, respectively. The video cameras were placed in front of the tank, as shown in the right photo of figure 1, and focused to minimize perspective errors in the images. Additional test visualizations with lateral views have been performed to check the two-dimensionality of the flow. Figure 2 gives experimental (photos) and numerical (solid lines) snapshots of the free surface for the case with $A/L = 0.10$, $T/T_1 = 1.39$ and $h/L = 0.40$. Here T_1 is the linear natural period of the tank. For the chosen parameters this case corresponds to the finite water depth regime. The results fit well with each other but for a minor phase shift. They show the occurrence of large water rise up along the side walls (top plots), water impacts against the wall with formation of air cushion (left-bottom plot) and the development of wave breaking phenomena (right-bottom plot).

Both experimentally and numerically, a systematic parametric analysis has been carried out in terms of excitation period, excitation amplitude and filling level of the tank. The period T has been varied between $0.8 T_1$ and $1.4 T_1$ and the

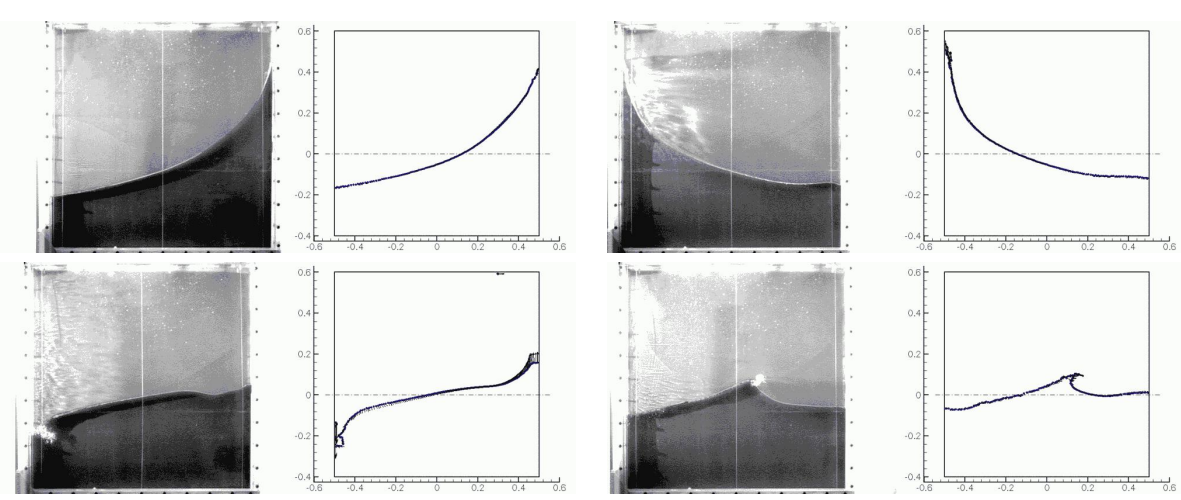


Figure 2: Free-surface evolution for $A/L = 0.10$, $T/T_1 = 1.39$ and $h/L = 0.40$. Present experiments (left photos) and SPH calculations (right free surfaces). Time increases from left to right and from top to bottom. The shown time instants are $t = 1.01, 1.41, 1.79$ and $2.68 T$.

corresponding resonance features have been analyzed. Values of A within $[0.03L; 0.10L]$ have been tested and nonlinear flow mechanisms have been examined. Finally the filling level h was increased from $0.125L$ to $0.50L$ and the influence on the resulting sloshing phenomena for fixed T and A have been investigated. Within the experimental program, a first stage considered a preliminary study to identify the different flow regimes and detect cases with relevant slamming occurrence. Flow visualizations with low speed video camera and water level measurements were realized. The second stage is presently in progress. It aims to study, more in details, the most relevant cases identified previously. In this phase, flow visualizations with high speed video camera and pressure measurements are performed. Left and right plots of figure 3 show our numerical and experimental maximum wave height (ζ) in the tank (probes at $0.05L$ from the side walls) as a function of the excitation period, for filling height $h = 0.35L$ and for oscillation amplitudes $A = 0.05L$ and $0.1L$, respectively. In the numerical simulations, the forced oscillation amplitude increases smoothly in time and reaches

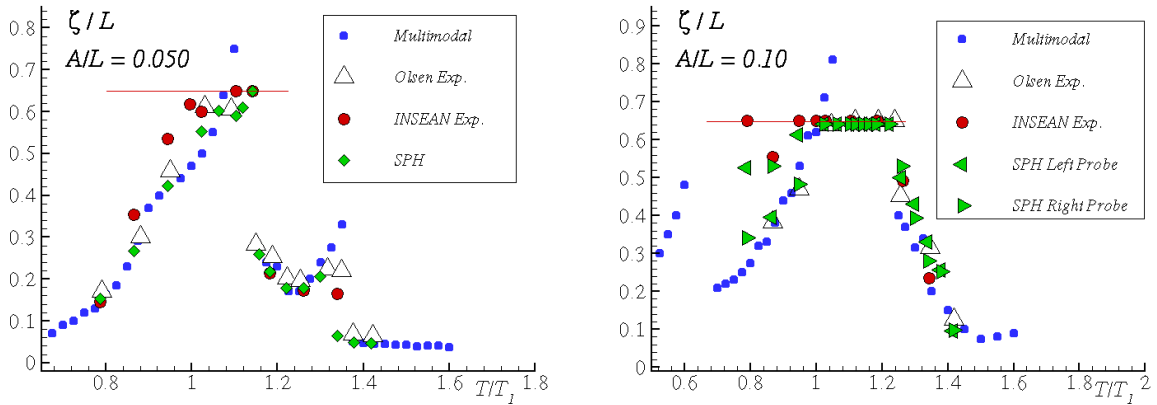


Figure 3: Maximum wave height in the tank (ζ) as a function of the excitation period. Excitation amplitude $A = 0.05L$ (left) and $A = 0.10L$ (right). Filling height $h = 0.35L$.

its steady-regime value in $10 T$. The simulation continues for about $30 T$ and the maximum wave elevation is recorded during the last ten periods of oscillation. The horizontal line in the plots indicates the roof, therefore the maximum wave height cannot exceed it and if it reaches such value, roof impacts occur. According to our measurements, for the chosen h , $A = 0.05L$ corresponds almost to the smallest excitation amplitude causing roof impacts. These events occur for a narrow range of excitation periods slightly above T_1 . For the largest A here shown, a wider number of excitation periods is able to determine such slamming events. The ζ -curves evidence the typical behavior with maximum water height amplified near the linear excitation period and progressively decreasing going far from this. In the plots, our experimental and numerical results are also compared with the experiments by Olsen (1970), where the same tank dimensions were considered, and with the multi-modal technique developed by Faltinsen *et al.* (2000). The theoretical method is not able to predict roof impacts and cannot handle free-surface breaking events. Apart from this and except for some localized discrepancies, all the results are in good agreement. This confirms the quality of present experiments and the validity of our numerical method.

Presently we are investigating the occurrence of slamming loads in the case of the smallest excitation amplitude here shown. Left plot of figure 4 gives the pressure evolution at probe P6 on the left side wall (see right photo) for $A/L = 0.05$,

$h/L = 0.35$ and $T/T_1 \simeq 1.107$. This case is characterized by large water rise up and gentle roof impacts. No relevant air

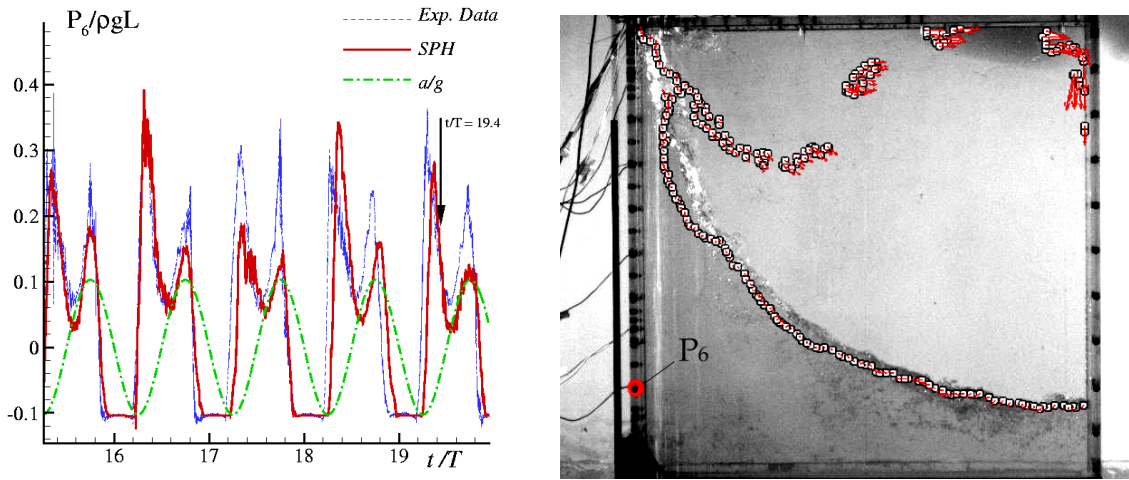


Figure 4: Case with $T/T_1 \simeq 1.107$, $A/L = 0.050$ and $h/L = 0.35$. Left: pressure evolution at probe P6 along the side wall (see right photo). Right: experimental water configuration during the roof impact. SPH free-surface particles are superimposed to the photo. The time instant is $t = 19.4T$ and the corresponding wall pressure is indicated by the arrow in left plot.

cushioning nearby or onto the side walls has been observed. It is then relevant to assume Froude scaling for the pressures. The slamming phenomenon at the roof is shown in the right of the figure. SPH free-surface particles are superimposed to the experimental photo and fit well the model test behavior. The probe pressure at this time instant is indicated by the arrow in the left plot where globally the measured pressure curve (dashed thin line) fairly compares with the SPH calculations (solid thick line). The pressure results show almost a periodic behavior with two pressure peaks in each

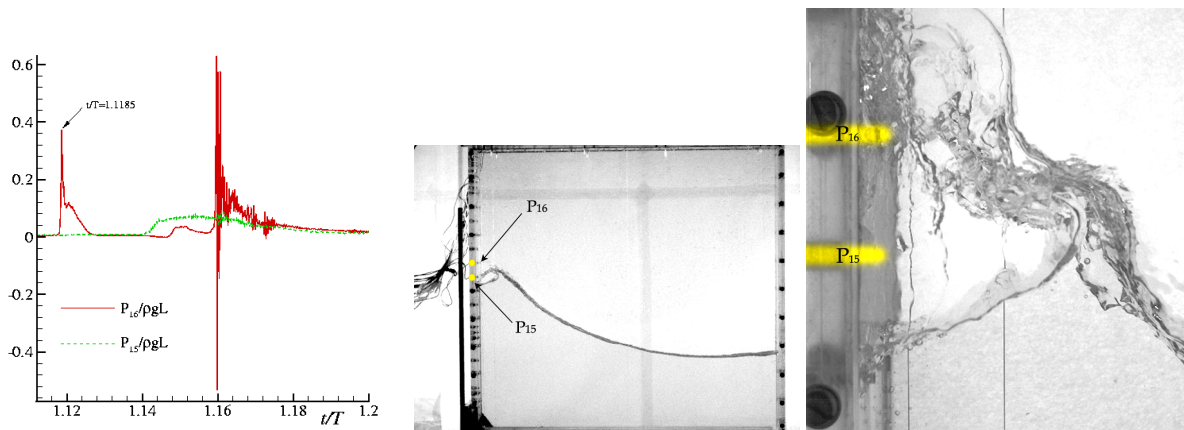


Figure 5: Case with $T/T_1 \simeq 0.869$, $A/L = 0.050$ and $h/L = 0.35$. Left: pressure evolution at probes P15 and P16 along the side wall (see center and right photos). Center : free surface during the jet impact against the side wall. An air cushion is created. Right: enlarged view of the air cavity.

period. The first peak occurs at the largest negative acceleration of the tank (dash-dotted line in the plot), when this has the maximum displacement on the left. Therefore, the peak is connected with the initial impact of the water on the side wall. The roof impact occurs slightly later, as shown by the arrow for the fifth period of the evolution reported in the left plot of figure 4. The second peak is of the same order of magnitude and appears after the roof impact, when the falling water hits the underlying liquid. In the considered case, this occurs almost when the tank has the maximum displacement on the right. The observed pressure behavior is consistent with the time evolution measured by Walkden and reported in Peregrine (2003) within the study of breaking waves impacting against vertical breakwaters. Peregrine refers to the curve as the typical impact profile measured in the tests in case of violent wave impacts and names it as "church roof" profile due to the double-peak behavior. The first peak is explained by the initial water-wall impact and the second one by the later water fall down under the gravity effects.

Left plot of figure 5 gives the pressure evolution at probes P15 and P16 along the side walls (shown in the center and right photos) for $A/L = 0.05$, $h/L = 0.35$ and $T/T_1 \simeq 0.869$. In this case no roof impact was recorded during the tests, while breaking wave phenomena were observed in the close neighborhood of the side wall, with the formation of air entrainment (see center and right photos). This means the Froude scaling is not valid anymore for the pressures. The compression of the air in the cavity is governed by the Euler number which should be accounted for. The used pressure gauges are in the wall area affected by the impact and by the further air cushioning. The occurrence of air entrainment can strongly influence the maximum value and the temporal variation of the structural loads (*cf.* Colagrossi

and Landrini (2003)) therefore a deep dedicated investigation is worth, although challenging to perform. Our pressure curve at P16 shows two peaks. The first one is connected with the initial impact of the plunging jet against the wall. The air compression in the subsequent enclosed cavity does not cause any substantial pressure increase. This is due to a three-dimensional behavior of the entrapped air which escapes laterally from the cavity. The later burst of the cavity is responsible of the second pressure peak and generates bubbly cloud pumping the surrounding flow. This explains the high frequency oscillations observed later in the pressure curve. Both the initial water-wall impact and the further cavity burst do not interest directly the lower probe P15 (5 cm below P16). In this case, the recorded local load is not affected by any significant peak.

The ongoing experimental investigations will examine the most relevant cases identified during the first stage of the research and will cover the different excitation amplitudes and filling heights previously considered. Attention will be paid to very peculiar events highlighted during the tests. For instance, for the largest A here considered, the major discrepancies in the maximum water height results (see right plot of figure 3) are observed for two excitation periods smaller than T_1 . One of these cases ($T = 0.787 T_1$) showed asymmetric behavior during our numerical calculations. This has been confirmed by the flow visualizations and by the water level measurements. Left plot of figure 6 shows the corresponding experimental time histories of the water height near the left (dashed line) and right (solid line) side walls. During the first eighty periods a clear asymmetric behavior is evidenced by the tests. Near one of the side walls, say the

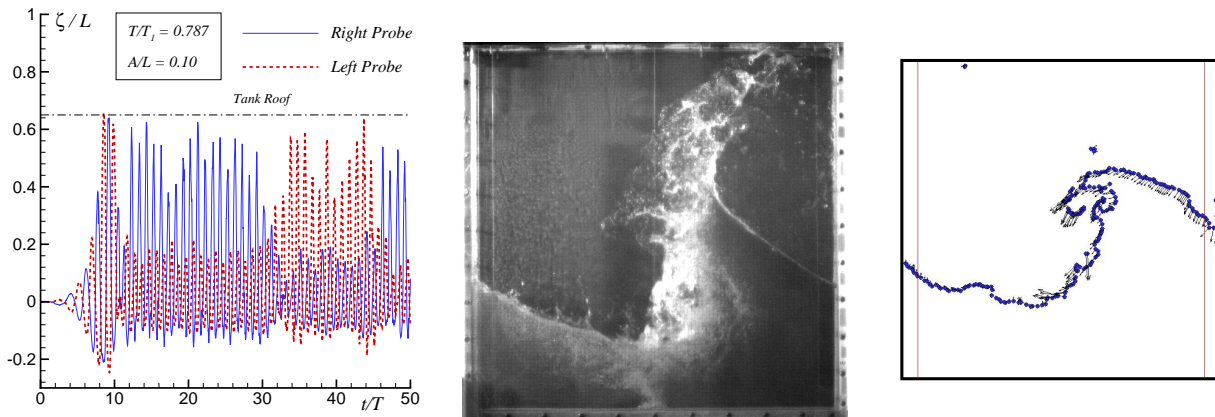


Figure 6: Example of asymmetric behavior in the tank for the case with $T = 0.787T_1$, $A = 0.10L$ and $h = 0.35L$. Left: wave height evolution near the left (dashed line) and right (solid line) side walls. Center and right: experimental (center) and numerical (right) free surfaces during the flow evolution. A massive water jump is observed.

left one, a strong free-surface deformation occurs creating a large jump (see experimental and numerical free surfaces in the center and right plots, respectively), collapsing against the side wall and originating a violent jet flow along the structure. The jet hits eventually the roof. Later on a large amount of water separates from the main mass in the form of a jet falling onto the underlying water. At this stage the liquid near the opposite wall reaches locally the maximum value, substantially smaller than at the left side. These phenomena last for several periods and are slightly affected by a phase delay due to nonlinear mechanisms. Eventually they disappear at the left side and start to occur on the opposite wall (see left plot of figure 6). The massive amount of energy involved in the slamming event could be the cause of the asymmetric behavior. A more detailed experimental analysis is needed and will be performed in the near future. The pressure measurements represent a good instrument to guide toward feasible explanations. The complex flow conditions occurring at the considered excitation period could partially explain the differences among the ζ results shown. The experimental program will be detailed described at the Workshop and the results will be analyzed in connection with SPH simulations. Relevance and challenges of performing pressure measurements in slamming flow regimes will be outlined.

The present research activity is partially supported by the Centre for Ships and Ocean Structures, NTNU, Trondheim, within the "Sloshing Flows and Related Local and Global Loads" project, and partially done within the framework of the "Programma di Ricerca sulla Sicurezza" funded by *Ministero Infrastrutture e Trasporti*.

References

- Monaghan J.J., 1994, "Simulating Free Surface Flows with SPH", *J. Comp. Phys.* **110**, pp. 399-406.
- A. Colagrossi and M. Landrini, 2003, "Numerical Simulation of Interfacial Flows by Smoothed Particle Hydrodynamics", *J. Comp. Phys.*, **191**, pp. 448-475.
- Olsen H., 1970, "Unpublished sloshing experiments at the Technical University of Delft", Delft, The Netherlands.
- Faltinsen O.M., Rognebakke O.F., Lukovsky I.A. and Timokha A.N., 2000, "Multidimensional modal analysis of nonlinear sloshing in a rectangular tank with finite water depth", *J. Fluid Mech.*, **407**, 201-234.
- Peregrine D.H., 2003, "Water-wave impact on walls", *Annu. Rev. Fluid Mech.*, **35**:23-43.

Discusser: H. Bredmose

Have you observed a variability of the wall pressures between transducers at the same horizontal level?

Author's reply:

The pressure transducers at the same level have been used to check the 2D evolution of the impact events involved. In general, the flow observed during the global experimental investigation was 2D. In the following figures 1-3 some examples are given both in shallow and in intermediate water depth. Each figure shows a snapshot of a phenomenon occurring in the tank (on the left) and the corresponding time evolution of the pressure recorded (on the center) by two sensors positioned at the same level. In particular, figure 1 is related to a lateral impact close to the transducers. Figure 2 gives a flip through phenomenon, and finally, figure 3 shows a classical church profile. For the first two cases, an enlarged view of the first peak in the pressure time history is also reported (right plot). All the cases evidence a rather 2D flow evolution. Some 3D effects are excited during the air cushioning phase (see right plot in figure 1) and during the formation of the jet at the wall in the flip through phenomenon (see right plot in figure 2); but in both cases they are very localised.

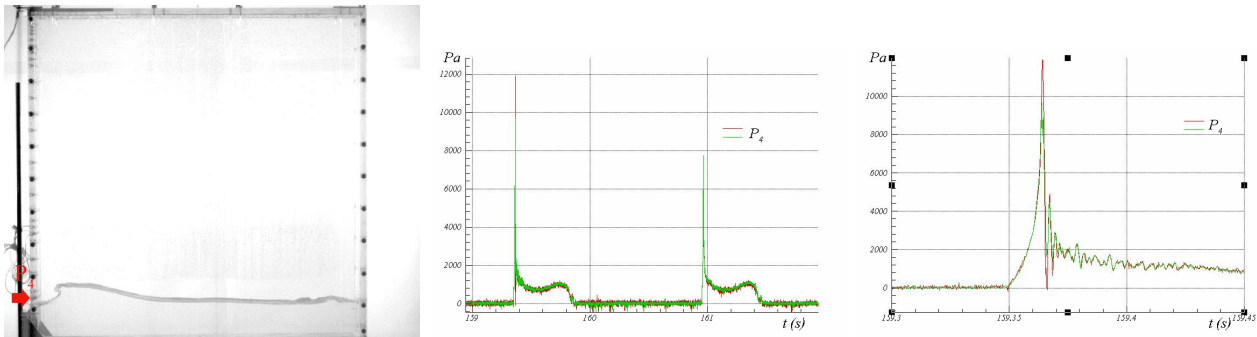


Figure 1: Example of the lateral impact flow ($h/L = 0.125$, $A/L = 0.03$, $T/T1 = 1$). Left: snapshot of the phenomenon. Center: time evolution of the pressure. Right: enlarged view of the first peak

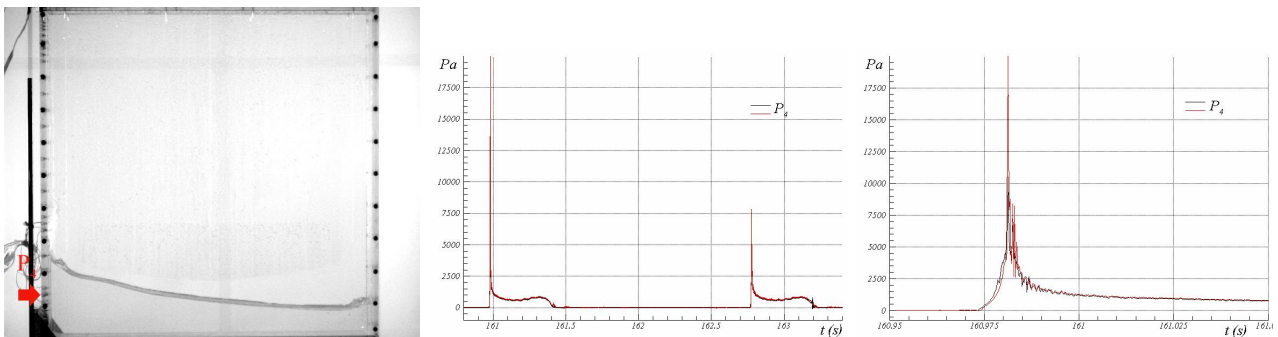


Figure 2: Example of the flip-through phenomenon ($h/L = 0.125$, $A/L = 0.03$, $T/T1 = 0.886$). Left: snapshot of the phenomenon. Center: time evolution of the pressure. Right: enlarged view of the first peak

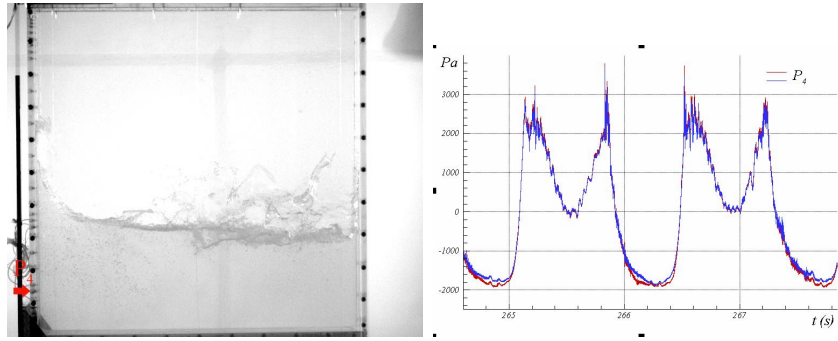


Figure 3: Example of the church profile ($h/L = 0.35$, $A/L = 0.07$, $T/T1 = 1.10$).
Left: snapshot of the phenomenon. Right: time evolution of the pressure.